Microcellular Foaming of PE/PP Blends

Ping Zhang, Nan Qiao Zhou, Qing Feng Wu, Ming Yi Wang, Xiang Fang Peng

Key Laboratory of Polymer Processing Engineering, Ministry of Education, National Engineering Research Center of Novel Equipment for Polymer Processing, South China University of Technology, Guanzhou 510640, China

Received 12 October 2006; accepted 6 December 2006
DOI 10.1002/app.26071
Published online in Wiley InterScience (www.interscience.wiley.com).

ABSTRACT: Three different polyethylene/polypropylene (PE/PP) blends were microcellular foamed and their crystallinities and melt strengths were investigated. The relationship between crystallinity, melt strength, and cellular structure was studied. Experimental results showed that the three blends had similar variation patterns in respect of crystallinity, melt strength, and cellular structure, and these variation patterns were correlative for each blend. For all blends, the melt strength and PP melting point initially heightened and then lowered, the PP crystallinity first decreased, and then increased as the PE content increased. At PE content of 30%, the melt strength and PP melting point were highest and the PP crystallinity was least. The blend with lower PP crystallinity and higher melt strength had better cellular structure and broader microcellular foaming temperature range. So, three blends had best cellular structure at PE content of 30%. Furthermore, when compared with PE/homopolymer (hPP) blend, the PE/copolymer PP (cPP) blend had higher melt strength, better cellular structure, and wider microcellular foaming temperature range, so it was more suited to be microcellular foamed. Whereas LDPE/cPP blend had the broadest microcellular foaming temperature range because of its highest melt strength within three blends. © 2007 Wiley Periodicals, Inc. J Appl Polym Sci 104: 4149–4159, 2007

Key words: polypropylene; polyethylene; blends; melt strength; microcellular foaming

INTRODUCTION

Polypropylene (PP) has wide application field in the packaging industry of food, cosmetic, and electron products[1] because of its low price, low density, good rigidity, high deformation recovery ratio as well as its super heat and chemical resistance, good degradability, and recyclability. Its application field will be widely broadened when PP microcellular foam products are produced successfully for the super properties of microcellular foams.

However, PP has poor foamability because of its high crystallinity and low melt strength because of its linear molecular structure and crystallinity property. In general, to produce foam products successfully, PP had to be modified. Physical blending modification with other material is simple, economical, and commonly used method. Amoco (Chicago, IL)[2] produced a foamed product having a density less than 0.2 g/cm^3, which was performed by blending a low viscosity polypropylene and high viscosity polypropylene to improve the cellular structure and decrease the foam density. Sumitom Chemical (Osaka, Japan)[3,4] produced a binding material having a good texture and high impact resistance by foaming a mixture of crystalline PP, noncrystalline PP, and low-density polyethylene (PE). A type of PP resin suitable to injection foaming was produced by blending PP with rubber particles of low glass transition temperature.[5]

In the recent years, Doroudiani et al.[6,7]and Rachtanapun et al.[8–10] made investigations on the microcellular foam processing for HDPE/PP blends, and studied the effect of crystallization and melt index on the cell morphology. They reported that the crystallinities of HDPE and PP decreased, the solubility of CO_2 in the polymer increased, and the microcellular structure of foamed samples was improved by blending PP with HDPE. The void fraction of foam was dependent on the HDPE-melt index. The higher the melt index, the higher the void fraction would be.[9] Nevertheless, adding PE to PP not only affected the crystallization but also had impact on the melt strength of the blends. The melt strength has strong relationship with the cell morphology and/or the cell collapse in microcellular foam processing, which has been studied only in brief. And PP or PE type might have an effect on the crystallinity and melt strength as well as the cell morphology, which has been lacked in the previous literatures. Furthermore, Doroudiani et al.[6,7] and Rachtanapun et al.[8–10] investigated the cell morphology of HDPE/PP blend using batch-foaming setup. The batch-foam processing characterized by long processing cycle time was not suited for industrialization.

Crystallinities and melt strengths of three PE/PP blends with different blend compositions were measured, microcellular foaming experiments were per-

Correspondence to: P. Zhang (cathyzp2002@163.com).
Contract grant sponsor: Chinese Ministry of Education; contract grant number: [01] 224,10,038.

Journal of Applied Polymer Science, Vol. 104, 4149–4159 (2007)

formed, and the relationship among the crystallinity, melt strength, and cell morphology was studied in this article. A self-designed dynamic simulation foaming setup was used to foam neat PP and PE/PP blends. The foam process, including heating, polymer melting, gas injecting, mixing, foaming, and cooling, using this dynamic foaming simulation setup is different from the batch-foam processing, but is similar to the extruding foam processing. Its experimental data have instructions to the extruding foaming. And it has many advantages over extruding foam processing including simple operation, easy processing control, and material saving. The experimental results showed that the crystallinity of PE/PP blend not only depended on the blend ratio of PE to PP, but also was related to the molecular architecture of blend component. The crystallinity and melt strength had great effect on the microcellular foamability. The blend with lower crystallinity and higher melt strength had better cellular structure and broader temperature range suited for microcellular foaming. Furthermore, the three blends had similar variation patterns in respect of crystallinity, melt strength, and cellular structure, and these variation patterns were correlative for each blend.

EXPERIMENTAL

Materials

Homopolymer polypropylene (hPP) and copolymer polypropylene (cPP) were used in this study. The hPP (T30S) was supplied by WuHan FengHuang (Wuhan, China) with melt flow rate of 0.8806 g/10 min (190°C, 2.16 kg). The cPP was supplied by Du Shan Zi Petrochemical, China, with melt flow rate of 0.533 g/10 min (190°C, 2.16Kg). The HDPE (5000S) and LDPE (18D) were commercial products from Da Qing Petrol Chemical (Daqing, China) with melt flow rates of 0.9 g/10 min and 1.751 g/10 min, respectively. Industrial-liquid CO_2 with purity of 99.5% supplied by GuangZhou JinZhu Chemistry (Guangzhou, China) was used as the foaming agent in this work.

Setup

A self-designed dynamic simulation foaming setup was used in this work. It consists of four main parts: a self-made supercritical fluid (SCF) supplier, which can supply supercritical CO_2 ($ScCO_2$) with a maximum pressure of 25 MPa and a maximum volume of 15 L, a drive set, an electromagnetic dynamic device, and a foaming unit. The foaming unit mainly consists of a rotor and foaming chamber, as shown in Figure 1. The rotor can circumferentially rotate and axially vibrate driven by the drive set and the electromagnetic dynamic device, which causes steady and dynamic shear force, respectively. Both steady and dynamic-foaming experiments can be carried out using this dynamic simulation foaming setup. The setup was designed originally to investigate the effect of superposition of axial vibration upon the steady shear force on the cell morphology. This article is the first part of the PE/PP microcellular foaming investigation work, and the rotor only circumferentially rotated without axial vibration in the foaming process. The differential scanning calorimetry (DSC204C, NETZSCH, Germany) and the scanning electron microscope (SEM XL30, Philip) were used to measure the crystallinity and observe the cellular structure.

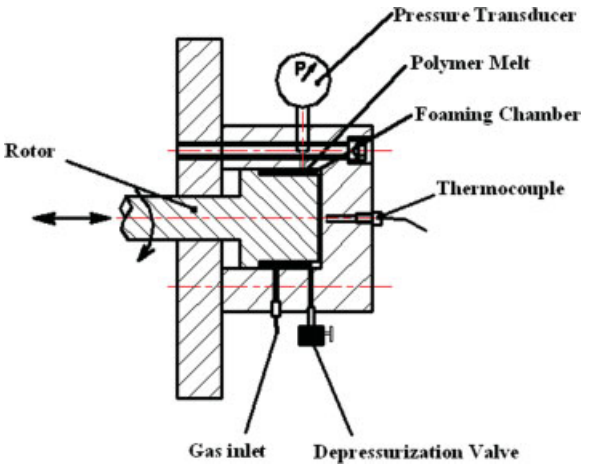

Figure 1 Schematic of foaming unit of the magnetic simulation foaming setup. [Color figure can be viewed in the online issue, which is available at www.interscience.wiley.com.]

Procedure

Blends preparation and property characterization

Blends of HDPE/hPP, HDPE/cPP, and LDPE/cPP at various PE to PP weight ratios (10 : 90, 20 : 80, 30 : 70, 40 : 60, and 50 : 50 w/w) were prepared using PLASTI-CORDER (BRABENDER, Germany) at 180°C. The crystallibilities were measured using DSC with a heating rate of 10°C/min. The crystalline fractions of PE and PP were calculated from the measured enthalpies of fusing for PE and PP, respectively. The detailed procedure was described in Ref. 7. The melt strengths were measured on a melt indexer (MP993A, Olsen, America) at 190°C, and the detailed procedure was shown in Refs. 11 and 12.

Microcellular foaming experiments

Neat PPs and PE/PP blends were shaped into ring-shaped samples similar to the size of the foaming chamber by using the Plane Sulfuration Machine (QLB-25D/Q, WuXi, China). The ring-shaped sample was put into the foaming chamber and heated to

TABLE I
Melting Point and Crystallinity of the HDPE/hPP Blend

HDPE : hPP	$T_{m,hPP}$ (°C)	χ_{hPP} (%)	$T_{m,HDPE}$ (°C)	χ_{HDPE} (%)
0 : 100	167.1	43.6		
10 : 90	166.1	32.2	130.9	41
20 : 80	166.5	31.3	131.3	43.7
30 : 70	167.2	29.9	133.8	46.9
40 : 60	165.3	30.06	132.5	52.0
50 : 50	164.5	30.3	134.5	55.5
100 : 0			134.8	58.0

$T_{m,hPP}$ and χ_{hPP} are the melting point and crystallinity of hPP in HDPE/hPP blend, respectively, and $T_{m,HDPE}$ and χ_{HDPE} are the melting point and crystallinity of HDPE in HDPE/hPP blend, respectively.

180°C. After equilibrium for 15 min, the rotor began to rotate and agitate the sample (the rotation speed was 65 rpm/min for all experiments) and the supercritical CO_2 was injected into the foaming chamber to a set-saturation pressure. Uniform polymer/gas solution was formed after CO_2 dissolved and diffused into the polymer melt under the action of shear force of the rotor. The rotor was stopped after rotating for 5 min. Then, the chamber was quickly depressurized by opening a depressurizaion valve when the melt temperature reached the set foaming temperature by cooling the chamber. The sudden supersaturation of CO_2 in the polymer-induced thermodynamic instability and plenty of cells began to nucleate and grow, and then solidified by cooling using a fan (the cooling rate remained invariable in all experiments). The cellular structure of ultimate foam was observed by taking SEM pictures after cooling and breaking in the liquid nitrogen.

RESULTS AND DISCUSSION

The melting points and crystallinities of HDPE/hPP, HDPE/cPP, and LDPE/cPP blends are tabulated in Tables I–III, respectively. Although the blends comprised different PP and PE, their crystallinities varied with increasing PE content in a similar pattern. For all blends, the PP melting point initially heightened and then lowered, the PP crystallinity first diminished, and then enhanced as the PE content increased. At PE content of 30%, the melting point was highest and crystallinity was least. The variation of the PE melting point with the increase of PE content was irregular, but tended to have a similar variation pattern with that of PP, whereas the PE crystallinity gradually increased as the PE content increased. The variation in crystallinization of PE/PP blends with PE content is contributed to the presence of materials in one phase having a pronounced effect on crystallization of material in the other phase. Park and coworkers[7] investigated the crystalline morphologies of HDPE/PP blend using a polarized optical microscope. They reported that the spherulite pattern of PP and HDPE crystals was changed and became irregular with blending, which led to the variation of melting points and crystallinities of PP and HDPE in the blend.

TABLE II
Melting Point and Crystallinity of the HDPE/cPP Blend

HDPE : cPP	$T_{m,cPP}$ (°C)	χ_{cPP} (%)	$T_{m,HDPE}$ (°C)	χ_{HDPE} (%)
0 : 100	168.3	37.1		
10 : 90	166.0	33.1	128.8	47.7
20 : 80	166.7	31.7	132.3	50.6
30 : 70	167.0	26.8	132.8	52.8
40 : 60	165.9	30.9	131.7	55.8
50 : 50	164.0	33.0	131.2	56.0
100 : 0			134.8	58.0

$T_{m,cPP}$ and χ_{cPP} are the melting point and crystallinity of cPP in HDPE/cPP blend, respectively, and $T_{m,HDPE}$ and χ_{HDPE} are the melting point and crystallinity of HDPE in HDPE/cPP blend, respectively.

TABLE III
Melting Point and Crystallinity of the LDPE/cPP Blend

LDPE : cPP	$T_{m,cPP}$ (°C)	χ_{cPP} (%)	$T_{m,HDPE}$ (°C)	χ_{HDPE} (%)
0 : 100	168.3	37.1		
10 : 90	167.3	37.0	107.2	22.6
20 : 80	167.7	36.1	107.2	24.3
30 : 70	168.7	35.2	108.6	25.8
40 : 60	166.3	35.7	108.4	27.9
50 : 50	166.2	36.8	109.2	29.2
100 : 0			111.1	30.0

$T_{m,cPP}$ and χ_{cPP} are the melting point and crystallinity of cPP in LDPE/cPP blend, respectively, and $T_{m,LDPE}$ and χ_{LDPE} are the melting point and crystallinity of LDPE in LDPE/cPP blend, respectively.

Melt strength

Figure 2 shows that the melt strength of HDPE/cPP blend was higher than that of HDPE/hPP blend possibly because of the difference in molecular compositions of the two blends. cPP is a copolymer of majority of propylene monomers and minority of ethylene monomers, which causes the enhancement in the miscibility and chain entanglement of PP and PE, leading to the increase of melt strength. Although hPP has poor miscibility with PE, because it is homopolymer of single propylene monomer that causes the low melt strength, the increase in melt strength by adding LDPE into cPP was larger than that by adding HDPE into cPP, likely because LDPE molecules involve a lot of long-chain branches. The long-chain branches enhance the chain entanglement and interaction of the two polymers, which caused higher melt strength of LDPE/cPP blend than that of HDPE/cPP blend.

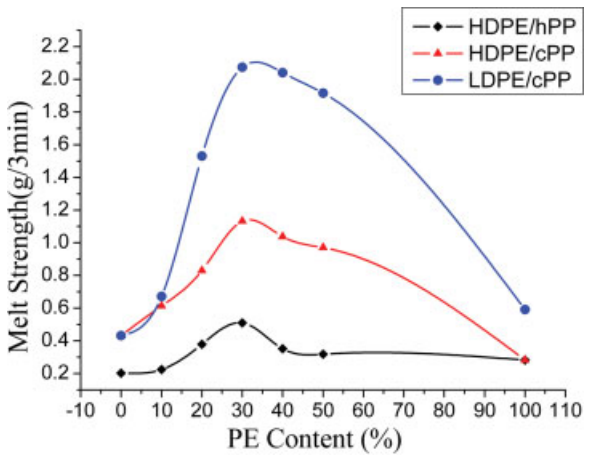

Figure 2 Melt strengths of HDPE/hPP, HDPE/cPP and LDPE/cPP blends as a function of PE content. [Color figure can be viewed in the online issue, which is available at www.interscience.wiley.com.]

Although the melt strengths of three blends were different, they followed the same variation rule with increasing PE content. Figure 2 shows the bell-shaped curve of melt strength for each blend. The melt strength initially enhanced and then diminished as the PE content increased, and reached its maximum value at PE content of 30%, which corresponded to the variation of crystallinity in previous section. So, it was considered that the variation rules of crystallinity and melt strength of PE/PP blends might be universal, regardless of PE and PP type.

The melt strength of blend was dependent on the miscibility of blend components.[11,13] Blends with completely miscibility or immiscibility showed no increase in melt strength, whereas those with partial miscibility demonstrated synergism in melt strength, leading to great enhancement in melt strength. And the blend miscibility varied with different blend ratio.[1] The melt strength was highest at the PE content of 30%, possibly because the 30 : 70 blend was the ratio with partial miscibility best suited for synergism in melt strength.

Microcellular foaming

Neat hPP and cPP and their blends with PE were foamed using the dynamic simulation foaming setup

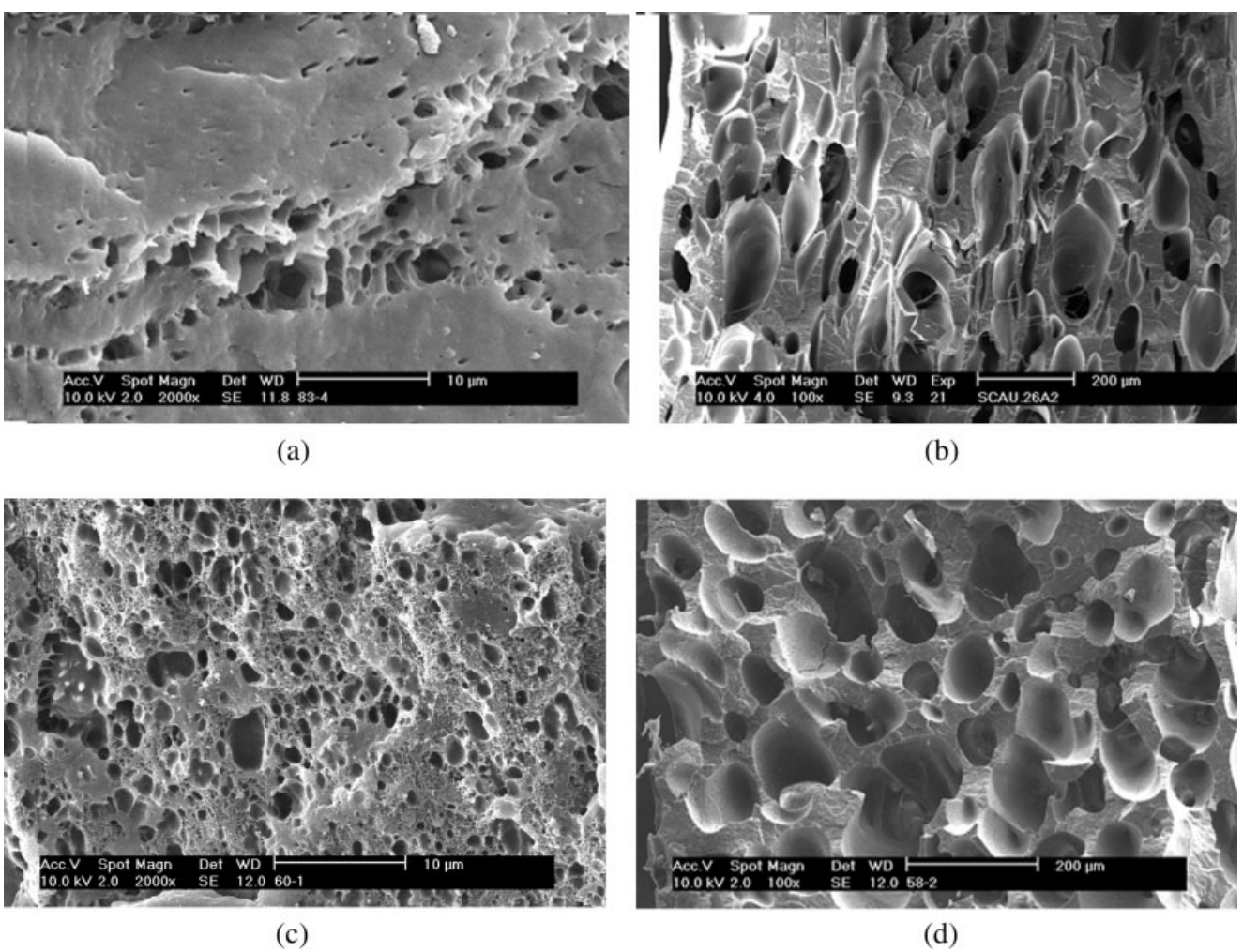

Figure 3 SEM micrographs of foamed neat hPP and cPP at 150 and 152°C under the saturation pressure of 12 MPa (a) hPP, 150°C; (b) hPP, 152°C; (c) cPP, 150°C; (d) cPP, 152°C.

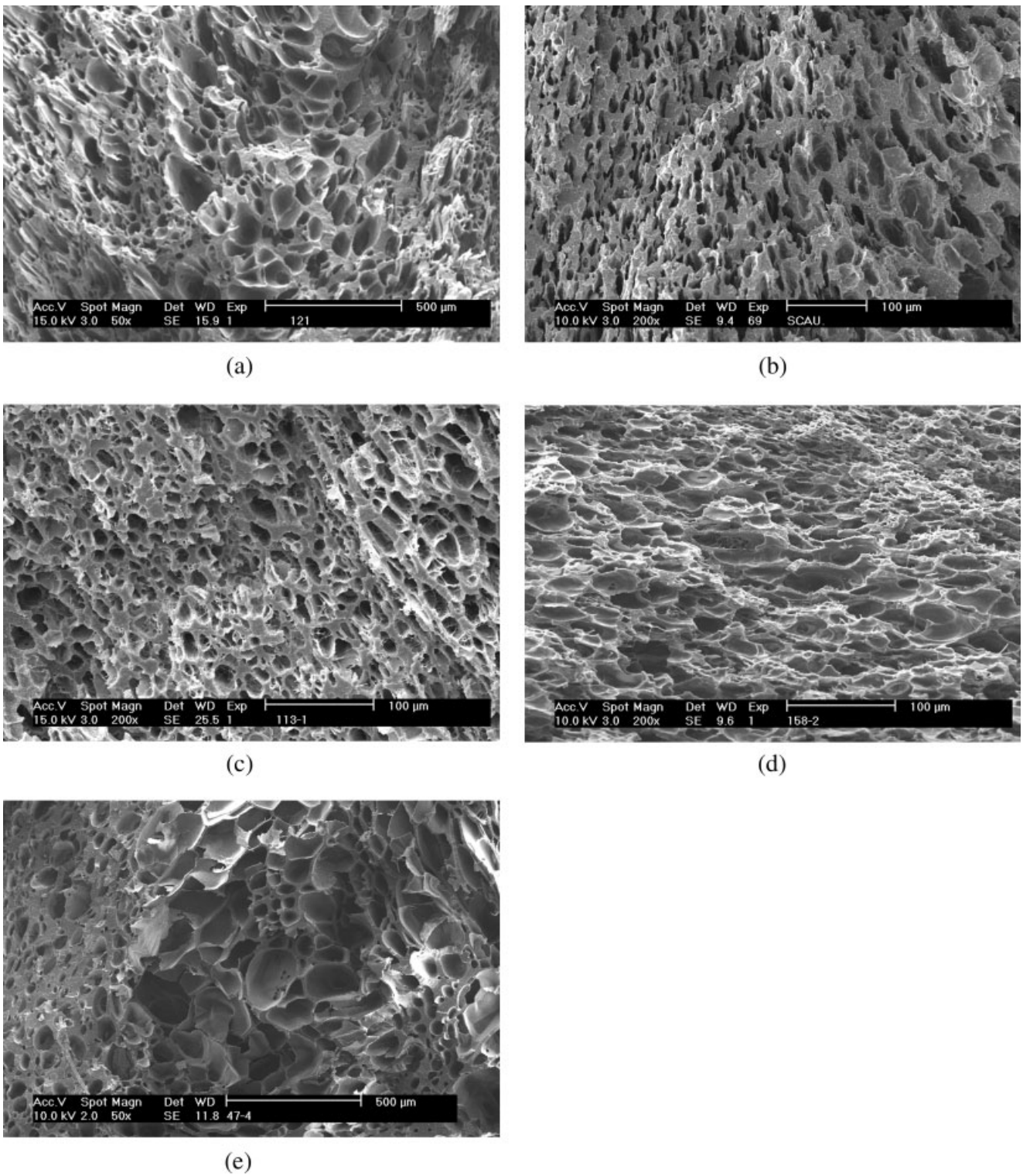

Figure 4 SEM micrographs of HDPE/hPP blend foamed at 150°C under the saturation pressure of 12 MPa (a) HDPE/hPP 10 : 90, (b) HDPE/hPP 20 : 80, (c) HDPE/hPP 30 : 70, (d) HDPE/hPP 40 : 60, and (e) HDPE/hPP 50 : 50.

and the cellular structures were scanned by SEM. Figure 3 shows that neat PP had very poor foamability. It was known from previous sections that the crystallinity and melt strength varied after blending PP with PE, which might influence the microcellular foamability. It is observed from Figures 4–9 that the cellular structures of foamed PE/PP blends were greatly improved in contrast to those of foamed neat PP. Furthermore, the blend with different PP and PE had different cellular structure. The cellular structures of

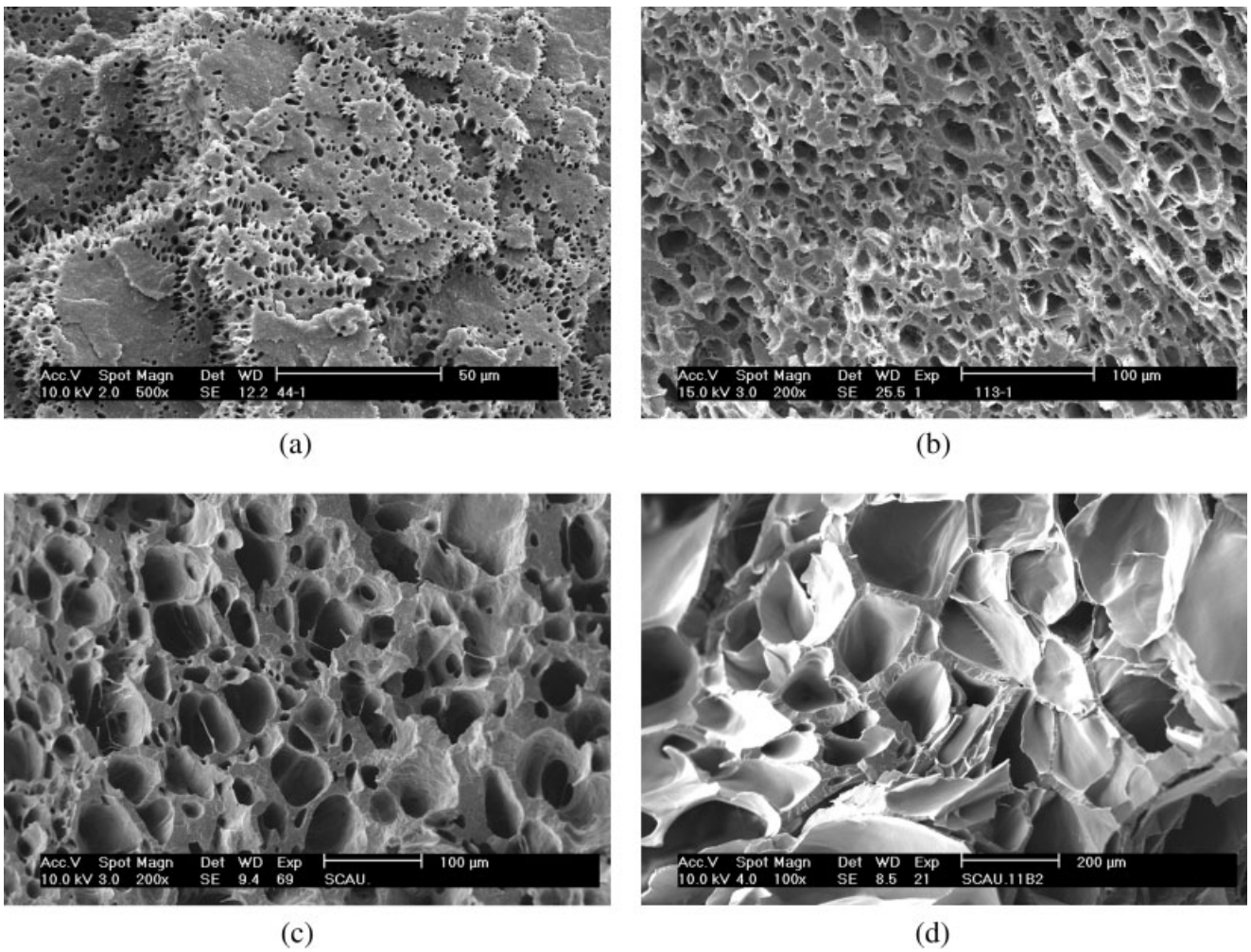

Figure 5 SEM micrographs of 30 : 70 HDPE/hPP blend foamed at various temperature under the saturation pressure of 12 MPa (a) 148°C, (b) 150 °C, (c) 152 °C, (d) 154 °C.

HDPE/hPP blend were irregular and cell-size distributions were nonuniform, as shown in Figures 4 and 5. But when cPP instead of hPP was blended with HDPE and was microcellular foamed, the cell morphology was greatly improved (Figs. 6 and 7). The reason is that cPP and HDPE has better miscibility because of the presence of ethylene monomers in cPP, which caused more uniform cell size and higher cell density in foamed HDPE/cPP blend. In addition, the higher melt strength of HDPE/cPP effectively restricted cell growth and retarded cell combination, leading to production of uniform and fine cellular structure. Figures 8 and 9 also show fine cell morphologies for foamed LDPE/cPP blend.

On the other hand, the cellular structure of blend was strong related to the PE content (Figs. 4, 6, and 8). The cell size decreased and cell-size distribution became more uniform as the PE content increased for all blends. But when the PE content was higher than 30%, the cell size began to increase and become less uniform. At PE content of 30%, the cellular structure was best with smallest cell size and highest cell density. The variation of cellular structure with PE content corresponded to those of crystallinity and melt strength.

Figures 5, 7, and 9 show the effect of foaming temperature on cellular structure. The cell size and cell density increased as foaming temperature elevated. The increased melt strength was beneficial to the increase of microcellular foaming temperature range. The blend with higher melt strength could be microcellular foamed in a broader foaming temperature range. For 30 : 70 HDPE/hPP, the temperature range suitable for microcellular foaming was very narrow and the cell size was easily beyond microcellular size, as shown in Figure 5. Whereas HDPE/cPP blend had broader microcellular foaming temperature range than that of HDPE/hPP blend because of its higher melt strength (Fig. 7). Figure 9 shows that the LDPE/cPP blend had widest microcellular foaming temperature range, which was contributed to its highest melt strength within three blends due to the long-chain branches in LDPE molecules.

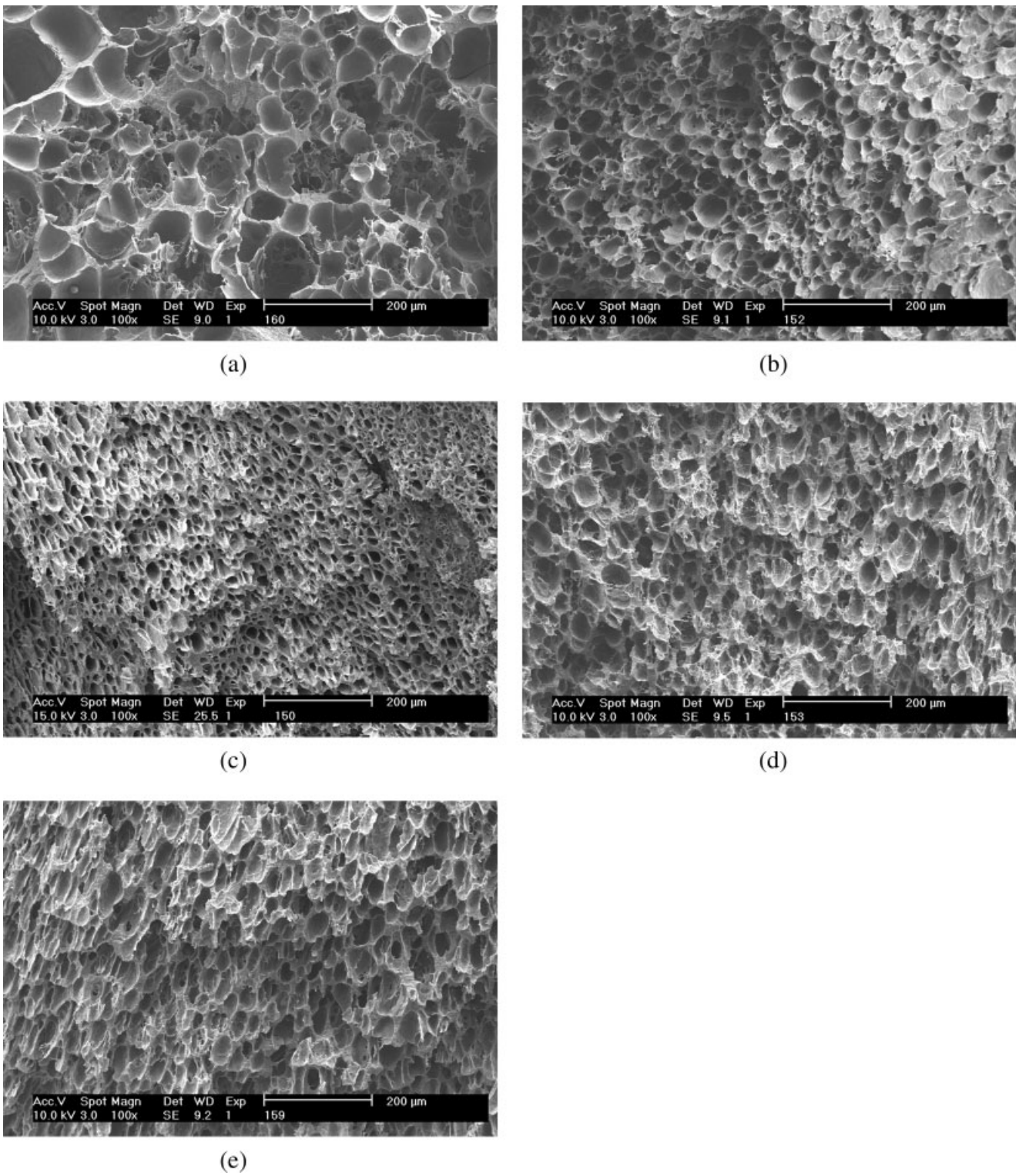

Figure 6 SEM micrographs of HDPE/cPP blend foamed at 150°C under the saturation pressure of 12 MPa (a) HDPE/cPP 10 : 90, (b) HDPE/cPP 20 : 80, (c) HDPE/cPP 30 : 70, (d) HDPE/cPP 40 : 60, (e) HDPE/cPP 50 : 50.

It is observed by comparing Figures 5, 7, and 9 with Tables I–III that the temperature range of 10–16°C lower than PP melting point was very suited for microcellular foaming. It was said that the polymer melt began to crystallize and the viscosity started enhancing when the melt temperature was depressed lower than the melting point. The lower the melt temperature, the more crystals presented in polymer and higher viscosity was induced, which led to more cells collapsing and more foaming difficulty. In this experi-

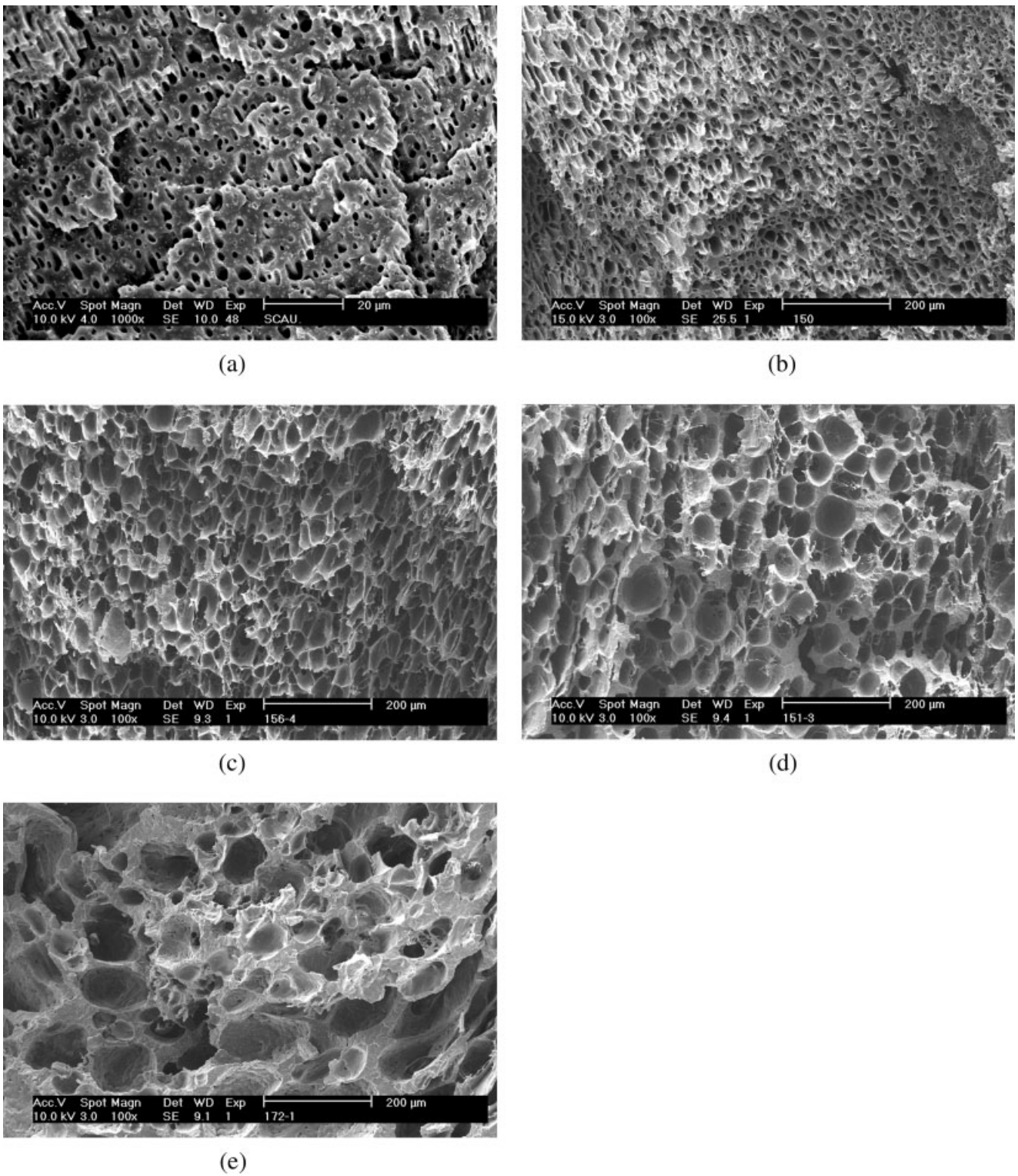

Figure 7 SEM micrographs of 30 : 70 HDPE/cPP blend foamed at various temperature under the saturation pressure of 12 MPa (a) 148, (b) 150, (c) 152, (d) 154, and (e) 156°C.

ment, however, the blends could be foamed in such a low temperature range, because the supercritical carbon dioxide (CO_2) was used as the physical foaming agent. The crystallization temperature (T_c) of polymer linearly lowered with CO_2 pressure when cooling at high CO_2 pressure.[14–17] The foaming temperature must be decreased with lowered T_c because semicrystalline polymer had appropriate melt viscosity and melt strength suited for microcellular foaming on condition that the foaming temperature was near T_c.

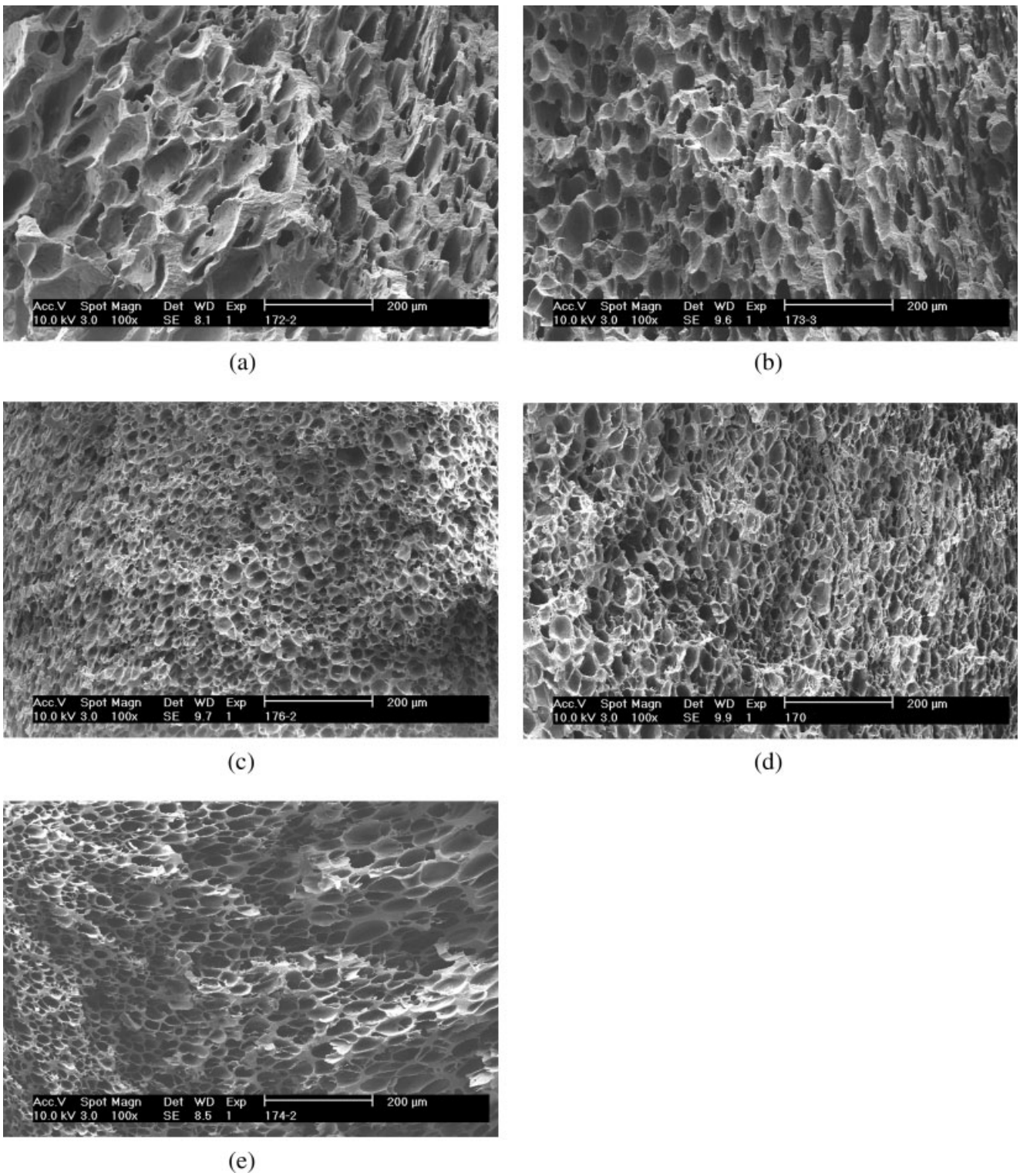

Figure 8 SEM micrographs of LDPE/cPP blend foamed at 150°C under the saturation pressure of 12 MPa (a) LDPE/cPP 10 : 90, (b) LDPE/cPP 20 : 80, (c) LDPE/cPP 30 : 70, (d) LDPE/cPP 40 : 60, and (e) LDPE/cPP 50 : 50.

According to Refs. 14 and 15, the foaming pressure of 12 MPa in this experiment could decrease T_c by around 15°C, so PE/PP blends could be foamed at such low temperature in this article.

CONCLUSIONS

The crystallinities and melt strengths of three PE/PP blends were measured, and the microcellular foaming experiments were performed using the microcellular

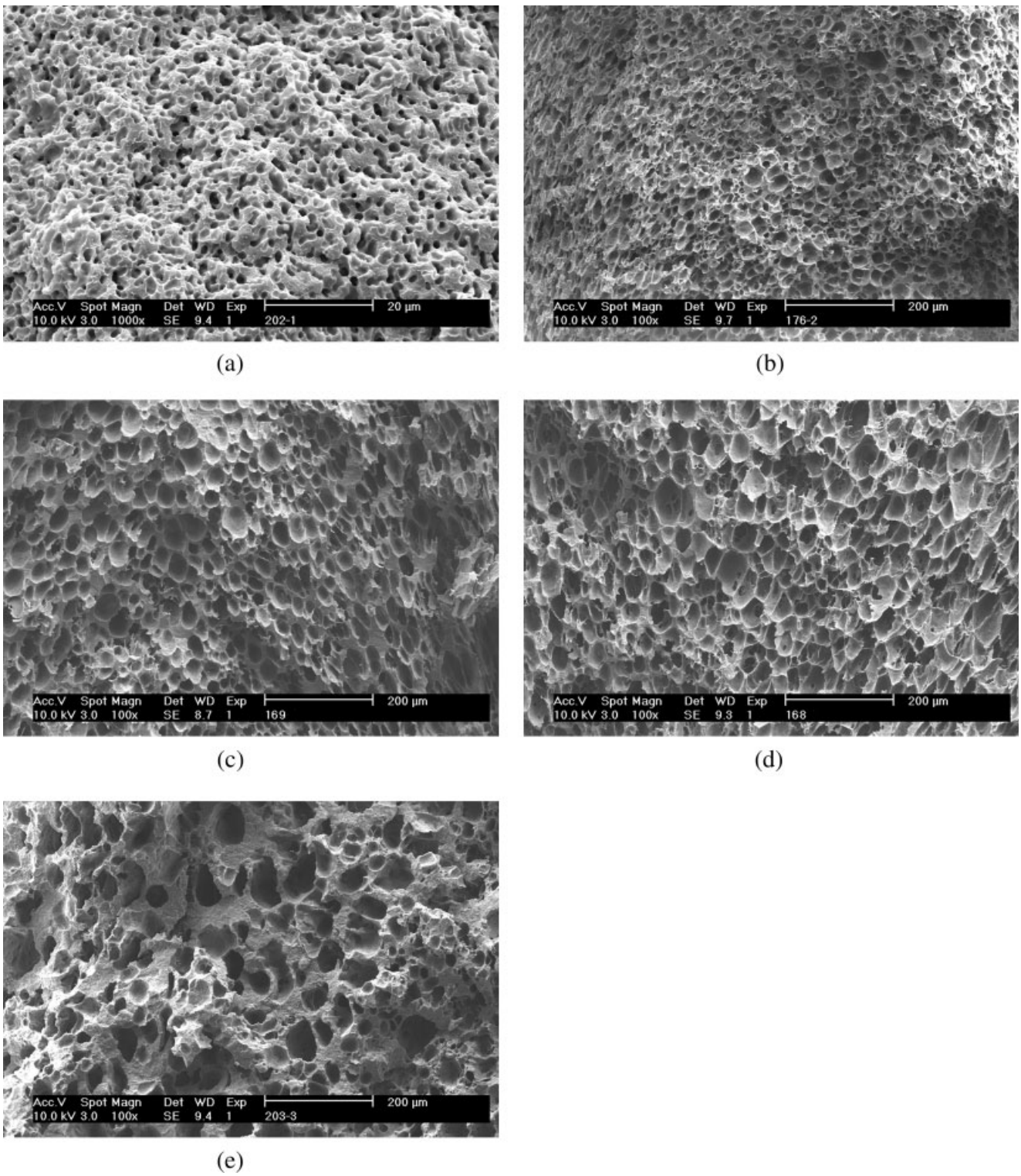

Figure 9 SEM micrographs of 30 : 70 LDPE/cPP blend foamed at various temperature under the saturation pressure of 12 MPa (a) 148, (b) 150, (c) 152, (d) 154, and (e) 156°C.

foaming simulatioin setup. On the basis of the experimental results, conclusions were made as follows:

1. The crystallinities of all blends had similar variation patterns with the PE content in some ways. The PP melting point initially heightened and then lowered, the PP crystallinity first decreased and then increased with the increase of the PE content. At PE content of 30%, the PP melting point was highest and crystallinity was least. The

PE melting point tended to have a similar variation pattern with that of PP, while the PE crystallinity gradually increased as the PE content increased.

2. For each PE/PP blend, the melt strength initially enhanced and then reduced with increase in PE content, and reached its maximum value at PE content of 30%, which corresponded to the variation rule of PP crystallinity. In addition, the melt strength of HDPE/cPP blend was higher than that of HDPE/hPP blend, but lower than that of LDPE/cPP blend.
3. The microcellular structure was strongly related to the crystallinity and melt strength. The blend with lower crystallinity and higher melt strength had better microcellular structure. The variation of cell morphology with PE content corresponded to those of crystallinity and melt strength for each blend. Initially, the cell size decreased and became more uniform as the PE content increased. Although the PE content was higher than 30%, the cell size increased and became less uniform. The cell size was smallest and cellular structure was best at PE content of 30%.
4. The temperature within the range of 10–16°C lower than PP melting point was suited for microcellular foaming for PE/PP blends. Higher foaming temperature led to larger cell size and lower cell density. Furthermore, the microcellular foaming temperature range of blends was broadened with increased melt strength. That is, the blend with higher melt strength could be microcellular foamed in a broader range of foaming temperature.

References

1. Zhao, M.; Gao, J. G.; Deng, K. L. New Polypropylene Resin by Modifying; Publishing Company of Chemical Industry: Beijing, 2002.
2. Alteepping, J.; Nebe, J. P. U.S. Pat. 4,940,736.
3. Ogawa, T.; Harada, T.; Ito, N.; Ohishi, K.; Nishibayashi, Y.; Shiozawa, K. U.S. Pat. 3,876,494.
4. Harada, T.; Ito, N.; Ohishi, K. U.S. Pat. 3,846,349.
5. Chengwang, C.; Cox, K. J Vinyl Addit Tech 1996, 2, 167.
6. Doroudiani, S.; Park, C. B.; Kortschot, M. T. Polym Eng Sci 1996, 36, 2645.
7. Doroudiani, S.; Park, C. B.; Kortschot, M. T. Polym Eng Sci 1998, 38, 1205.
8. Rachtanapun, P.; Selke, S. E. M.; Matuana, L. M. J Appl Polym Sci 2003, 88, 2842.
9. Rachtanapun, P.; Selke, S. E. M.; Matuana, L. M. J Appl Polym Sci 2004, 93, 364.
10. Rachtanapun, P.; Selke, S. E. M.; Matuana, L. M. Polym Eng Sci 2004, 44, 1551.
11. Ho, K.; Kale, L.; Montgomery, S. J Appl Polym Sci 2002, 85, 1408.
12. Zhan, G. R.; Zhou, N. Q.; Peng, X. F. China Plast 2003, 17, 79.
13. Field, G. J.; Micic, P.; Bhattacharya, S. N. Polym Int 1999, 48, 461.
14. Kishimoto, Y.; Ishii, R. Polymer 2000, 41, 3483.
15. Varma-Nair, M.; Handa, P. D.; Mehta, A. K.; Agarwal, P. Thermochim Acta 2003, 396, 57.
16. Takada, M.; Tanigaki, M.; Ohshima, M. Polym Eng Sci 2001, 41 1938.
17. Zhang, Z.; Day, M.; Nawaby, A. V. J Polym Sci Part B: Polym Phys 2003, 41, 1518.